ELSEVIER

Materials Science and Engineering A337 (2002) 222–227

MATERIALS SCIENCE & ENGINEERING A

www.elsevier.com/locate/msea

Microstructural studies of in-situ formed MgB_2 phases in a Mg alloy matrix composite

Y.X. Chen [a,*], D.X. Li [a], G.D. Zhang [b]

[a] *Laboratory of Atomic Imaging of Solids, Institute of Metal Research, Chinese Academy of Sciences, Shenyang 110015, People's Republic of China*
[b] *State key Laboratory of Metal Matrix Composites, Shanghai Jiao Tong University, Shanghai 200030, People's Republic of China*

Received 2 November 2001; received in revised form 3 January 2002

Abstract

The microstructure of in-situ formed MgB_2 phases in a Mg alloy matrix composite was studied by means of transmission electron microscopy and high-resolution electron microscopy. The MgB_2 phases have hexagonal plate-like morphology with a remarkable interfacial energy anisotropy. The interfaces between MgB_2 and Mg are sharp without any intermediate layer. The interfaces are semi-coherent with a regular arrangement of misfit dislocations. Dislocation loop and 60° dislocation are observed in the MgB_2 phases. A phase transformation from MgB_2 to Mg is observed and a structural model is proposed to describe the phase transformation process.

Keywords: MgB_2; Microstructure; Phase transformation

1. Introduction

It is well known that the microstructure of material has a close relation with its mechanical and physical properties. For metal matrix composites, a lot of works, concerning relations between the microstructure and the mechanical properties, had been conducted [1–7]. Among these works, high-resolution electron microscopy (HREM) has been widely used to study the interfacial , defect and grain boundary structures, which provides a useful way to investigate the microstructural feature under atomic scale [3–5].

Recently, a hybrid Mg alloy matrix composite reinforced with SiC whiskers and B_4C particles was fabricated. The SiC whisker is widely used as reinforcement in metal matrix composite because of its high strength and good corrosion resistance. B_4C particle has the lowest density among ceramic particles and is attempted to separate the SiC whisker uniformly in the composite. The composite has a very low density and exhibits very good mechanical properties [8]. The microstructure of the composite was investigated by means of HREM, which indicated that MgB_2 phases were formed during fabrication process of the composite [9]. The MgB_2 phase has a AlB_2-type structure with space group of $P6/mmm$ and lattice constants of $a = 0.3086$ nm, $c = 0.3522$ nm.

Recently, MgB_2 has attracted much attention [10], because of the discovery of superconductivity in the MgB_2 compound [11]. However, so far, few work concerning the microstructural features of the MgB_2 phase is reported in the literature. In this paper, the morphology, defects and phase transformation of the MgB_2 phase are studied by means of transmission electron microscopy (TEM) and HREM.

2. Experimental

ZK60A magnesium alloy was chosen as matrix alloy. The composition of the alloy is as follow (wt.%): 5.0–6.0 Zn, 0.3–0.9 Zr and the balance is Mg. SiC whiskers and B_4C particles were chosen as reinforcements. The hybrid composite was fabricated by means of liquid infiltration

* Corresponding author. Tel.: +81-22-217-7326; fax: +81-22-217-7325
E-mail address: yxchzh@yahoo.com (Y.X. Chen).

0921-5093/02/$ - see front matter
PII: S0921-5093(02)00033-3

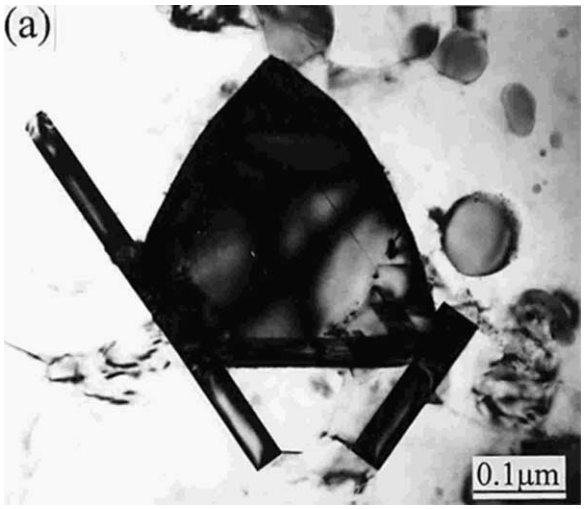

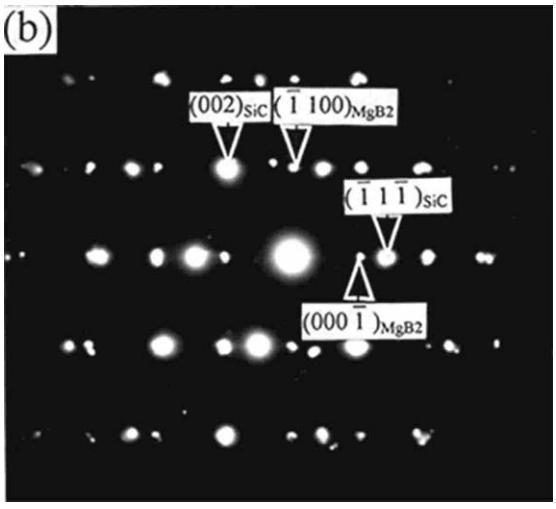

Fig. 1. (a) BF TEM image viewed along the [110] zone axis of SiC, showing two whisker-like phases at the SiC surfaces. (b) Corresponding SADP taken from SiC and one of the whisker-like phase.

method. First, SiC whisker and B_4C particles were mixed in a wet process and dispersed, and then were pressed to a preform by the addition of a suitable bonder. The preform was preheated and infiltrated by the ZK60A alloy melt under high pressure with protection of Ar gas. Finally, the composite was extruded.

TEM samples were prepared using conventional procedure. First, a disc was cut from the composite and then mechanically polished to a thickness of about 50 μm. After that, the disc was dimpled in the center to a thickness of about 20 μm, followed by ion-beam thinning to perforation. Ion-beam thinning was performed at 5 kV and an incident angle of 10°. TEM and HREM observations were performed with a JEM2000EXII high-resolution electron microscope.

3. Results and discussion

3.1. Formation and morphology of the MgB_2 phases

Fig. 1(a) is a bright field (BF) TEM image viewed along the [110] zone axis of SiC. The image reveals that two whisker-like phases are formed at the SiC surfaces with regular morphologies. Fig. 1(b) is the corresponding selected area diffraction pattern (SADP) taken from SiC and one of the whisker-like phases. The SADP indicates that the whisker-like phase is MgB_2 viewed along the $[11\bar{2}0]$ zone axis. Another phase formed at the SiC surfaces is MgO, which is a very thin layer, positioned between SiC and MgB_2 [9]. The combined information from Fig. 1(a and b) reveals that the long axis of the MgB_2 phase is along the $[2\bar{1}\bar{1}0]$ direction, while the short axis is along the [0001] direction.

During fabrication process of the composite, B_4C particles were heated to 700 °C. Thus, liquid B_2O_3 was formed at the surfaces of B_4C due to the low melting point of B_2O_3, i.e. 450 °C [12], through the chemical reaction,

$$B_4C + O_2 \rightarrow B_2O_3 + CO_2 \quad (1)$$

Some of the liquid B_2O_3 flowed over the surfaces of nearby SiC, and further reacted with liquid Mg,

$$B_2O_3 + Mg \rightarrow MgB_2 + MgO \quad (2)$$

As a result, MgB_2 and MgO were formed at the SiC surfaces.

Fig. 2 is a BF TEM image viewed along the [0001] zone axis of MgB_2. The corresponding SADP is inset in the image. The image exhibits faceted morphology of the MgB_2 phase. The six facets are coincident with the six $\{1\bar{1}00\}$ lattice planes of MgB_2. From the combined

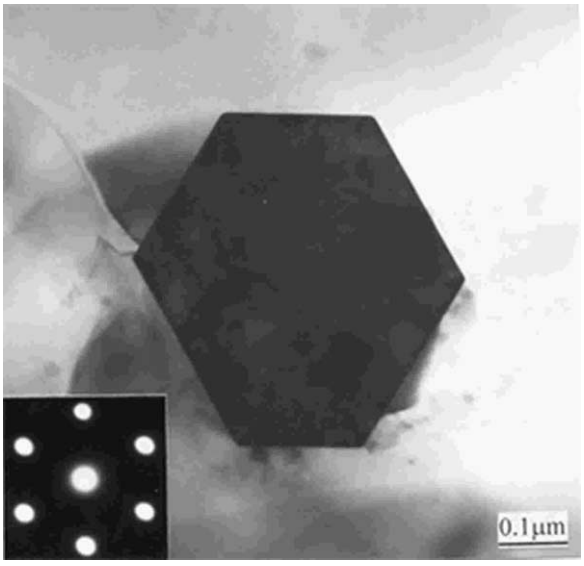

Fig. 2. BF TEM image viewed along the [0001] zone axis of the MgB_2 phase. The corresponding SADP is inset in the image.

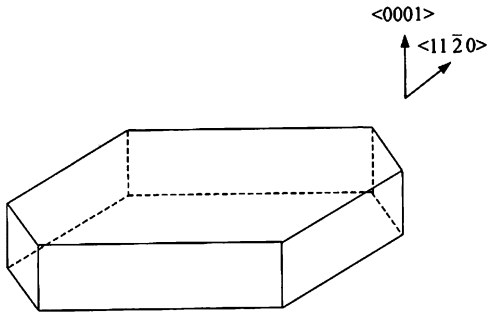

Fig. 3. Schematic drawing of the hexagonal plate-like morphology of the MgB_2 phase formed in the Mg alloy matrix.

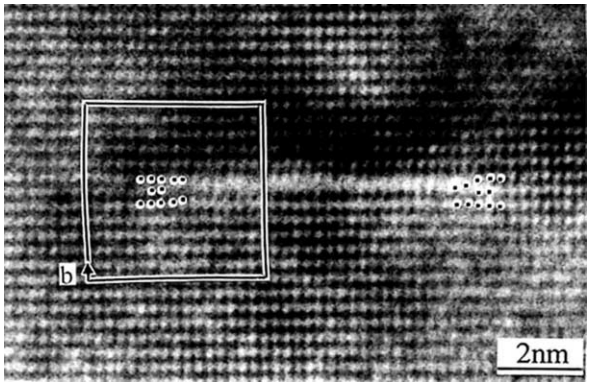

Fig. 4. HREM image viewed along the [11$\bar{2}$0] zone axis of MgB_2, exhibiting a dislocation loop in the MgB_2 phase.

information of Fig. 1(a) and Fig. 2, it is concluded that the MgB_2 phase has a hexagonal plate-like morphology in the Mg alloy matrix. A schematic drawing of the MgB_2 morphology is shown in Fig. 3.

It is well known that, for a crystal in the equilibrium state, the ratio of interfacial energy to spacing between interfaces and symmetric center is a constant. Namely, $\gamma_i/h_i = \text{constant}$, where γ_i and h_i denote the interfacial energy and the spacing between the interfaces and the symmetric center of the crystal, respectively. From Fig. 3, it can be seen that, in the Mg alloy matrix, the MgB_2 phase has a remarkable interfacial energy anisotropy. The {0001} interface has the lowest energy. The growth direction of the MgB_2 phase is the close-packed $\langle 11\bar{2}0 \rangle$, instead of $\langle 0001 \rangle$.

3.2. Defects in the MgB_2 phases and the interfaces between the MgB_2 phases and the Mg alloy matrix

Fig. 4 is an HREM image viewed along the [11$\bar{2}$0] zone axis of MgB_2, which exhibits a dislocation loop present in the MgB_2 phase. The dislocation loop is along the close-packed {0001} lattice plane of MgB_2. In order to determine the Burgers vector of the defect, a Burgers circuit is drawn around one side of the dislocation loop. From the Burgers circuit, it can be seen that the Burgers vector of the dislocation loop is [0001], which is a Burgers vector of a perfect defect. However, since the

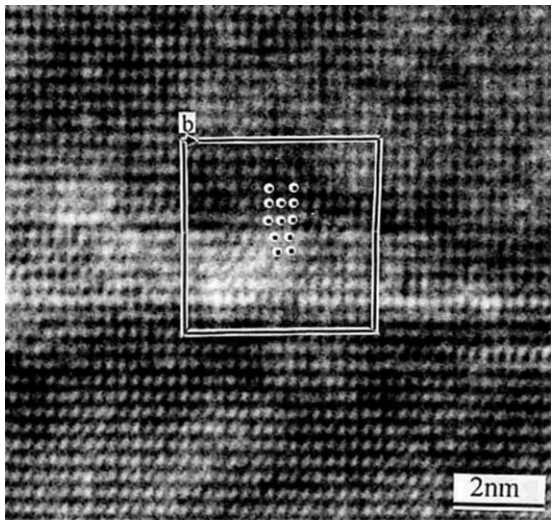

Fig. 5. HREM image viewed along the [11$\bar{2}$0] zone axis of MgB_2, exhibiting a dislocation in the MgB_2 phase.

Burgers vector is perpendicular to the {0001} sliding planes, the dislocation loop cannot slide along the {0001} planes.

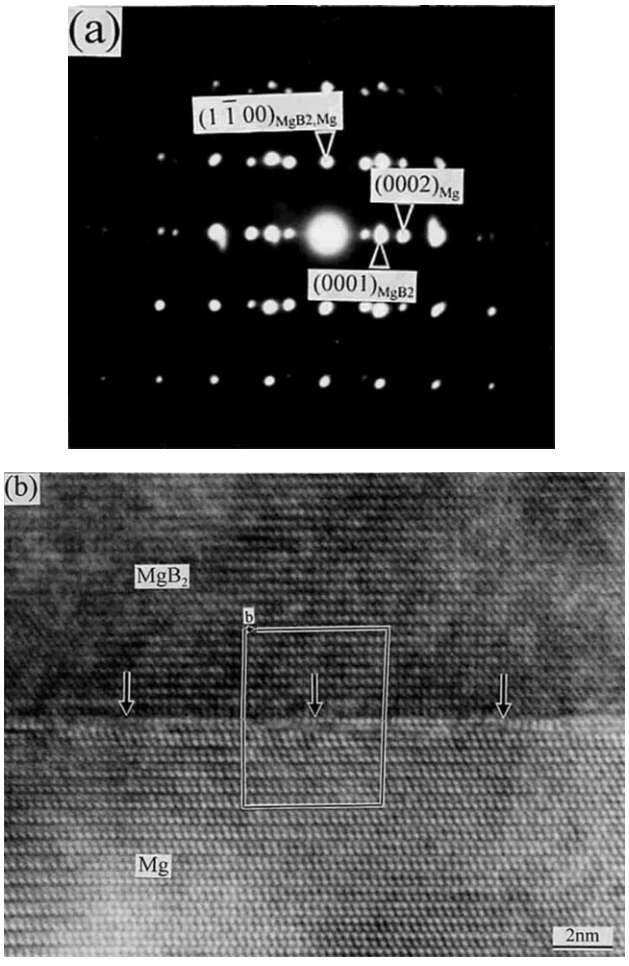

Fig. 6. (a) SADP taken from MgB_2 and Mg. (b) Corresponding HREM image showing the interfacial features.

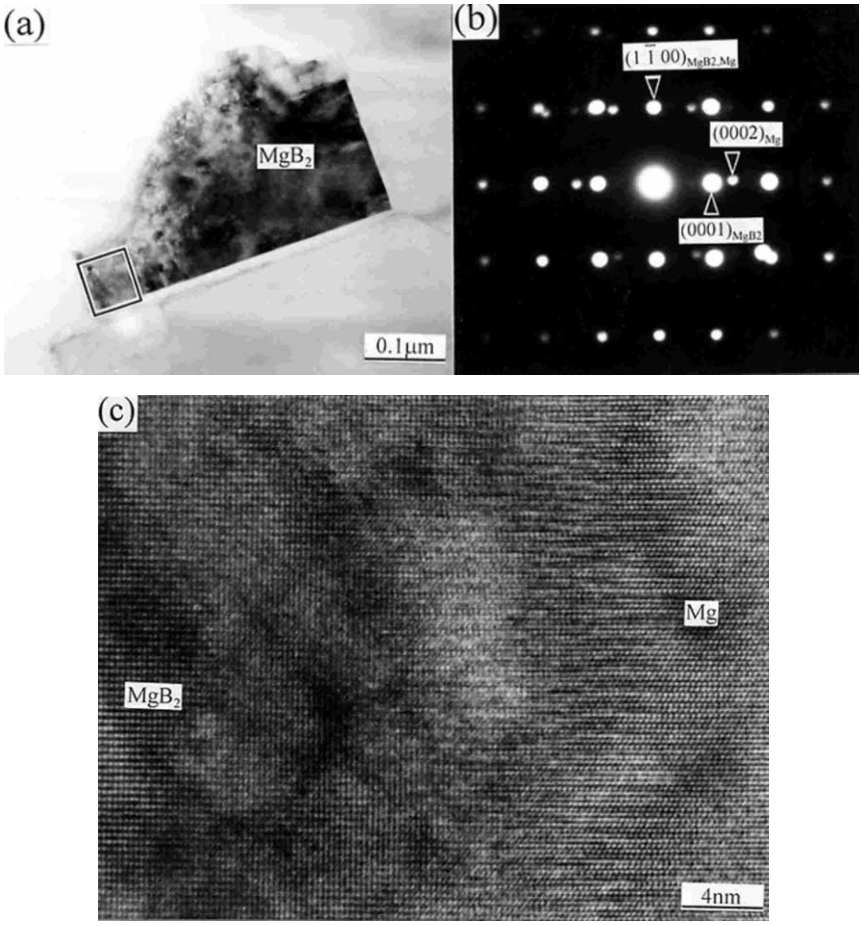

Fig. 7. (a) BF TEM image showing a MgB_2 phase at the edge of TEM sample. (b) SADP taken from the outlined area shown in (a). (c) Corresponding HREM image.

In addition to the dislocation loop, dislocations are also observed in the MgB_2 phases. Fig. 5 is an HREM image taken along the $[11\bar{2}0]$ zone axis of MgB_2, which shows a dislocation present in the MgB_2 phase. The Burgers circuit around the dislocation indicates that the projected Burgers vector is $1/2[1\bar{1}00]$, which is a Burgers vector of a partial dislocation. Thus, the actual Burgers vector should be $1/3[2\bar{1}\bar{1}0]$. The projection of $1/3[2\bar{1}\bar{1}0]$ on the $(11\bar{2}0)$ lattice plane is $1/2[1\bar{1}00]$, which is the edge component of the Burgers vector. Namely, the dislocation is a 60° dislocation.

Fig. 6(a) is a SADP taken from MgB_2 and Mg, which establishes an orientation relationship between the two phases, i.e.

$$[11\bar{2}0]_{MgB_2} \| [11\bar{2}0]_{Mg}$$

$$(0002)_{MgB_2} \| (0002)_{Mg}$$

The close-packed lattice plane and direction of MgB_2 and Mg are parallel with each other. Fig. 6(b) is the corresponding HREM image, showing the interfacial features. From the HREM image, it can be seen that the (0001) interface between MgB_2 and Mg is sharp without any intermediate layer. Misfit dislocations (indicated by black arrows) are present at the interface to accommodate the lattice mismatch between the two phases. The half lattice planes of the misfit dislocations are positioned at the MgB_2 side of the interface. The arrangement of the misfit dislocations is regular with an average spacing of $22.5d$ (d denotes the $\{1\bar{1}00\}$ lattice spacing of MgB_2). A Burgers circuit is drawn around one of the misfit dislocations. From the Burgers circuit, it can be seen that the Burgers vector of the misfit dislocation is $1/2[1\bar{1}00]$. This Burgers vector is associated with a partial dislocation. Thus, the actual Burgers vector is $1/3[2\bar{1}\bar{1}0]$. The edge component of the Burgers vector, i.e. $1/2[1\bar{1}00]$, contributes to accommodation of the lattice mismatch between MgB_2 and Mg. The lattice misfit parameter, δ, can be calculated by the equation:

$$\delta = \frac{2(a_1 - a_2)}{a_1 + a_2}, \tag{3}$$

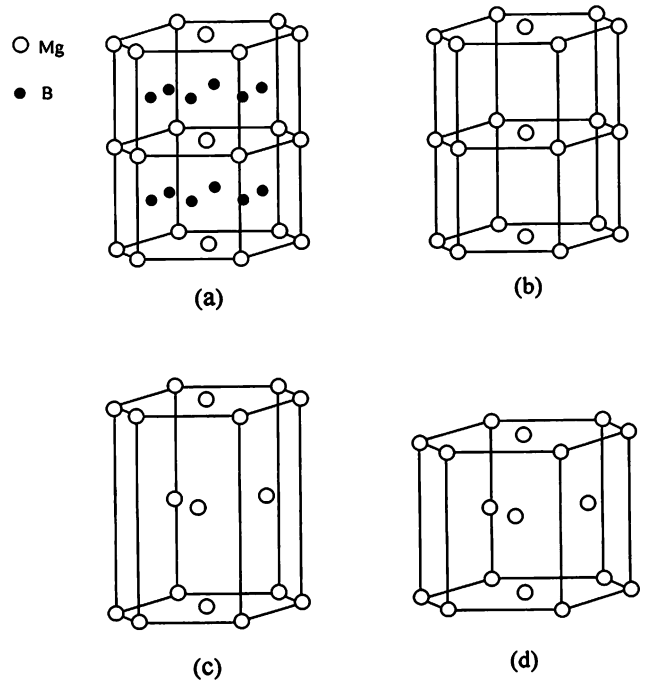

Fig. 8. Schematic drawing of a structural model describing the phase transformation process. (a) A supercell composed of two unit cells of MgB_2. (b) A supercell formed after 12 B atoms escape from the supercell shown in (a). (c) A supercell formed after the Shockley partial dislocation slides across the {0002} lattice plane of the supercell shown in (b). (d) Unit cell of Mg.

where a_1 and a_2 denote lattice constants of MgB_2 and Mg, respectively. The calculated lattice misfit, δ, is 3.9%. The spacing between the misfit dislocations can be calculated by the equation:

$$D = \frac{b}{\delta}, \tag{4}$$

where b denotes edge component of the Burgers vector, i.e. $1/2[1\bar{1}00]$. The calculated spacing is $19.7d$, which is smaller than the experimental value, i.e. $22.5d$. It is therefore expected that there is still 13% elastic strain remaining at the interface. Similar observations have been reported in many works [13,14].

3.3. Phase transformation from MgB_2 to Mg

Fig. 7(a) is a BF TEM image showing a MgB_2 phase at the edge of TEM sample. Fig. 7(b) is a SADP taken from the outlined area shown in Fig. 7(a). The SADP exhibits a superimposition of diffraction patterns from MgB_2 and Mg along the common $[11\bar{2}0]$ zone axes. Fig. 7(c) is the corresponding HREM image of the outlined area shown in Fig. 7(a). The HREM image reveals a gradual transition from the MgB_2 lattice to the Mg lattice, which is much different from the interfacial features between MgB_2 and Mg shown in Fig. 6(b). It is thus concluded that a phase transformation from MgB_2 to Mg is happened in this area. By taking every aspect into account that may induce this phase transformation during preparation of the TEM samples, we consider that a possible reason for the phase transformation should be due to Ar^{2+} ions bombardment during ion-bean thinning of the TEM samples. The light B atoms in the MgB_2 lattice might obtain enough energy to escape from the MgB_2 lattice by the bombardment of the Ar^{2+} ions. Consequently, the phase transformation from MgB_2 to Mg is occurred.

A structural model is proposed to describe the phase transformation process, which can be divided into three steps. It should be noted that this division into three steps is only for convenience of description, and does not means the actual process of the phase transformation.

1) First, it is supported that a supercell composed of two MgB_2 unit cells is present, as shown in Fig. 8(a). Because of the Ar^{2+} ions bombardment during ion-bean thinning of the TEM samples, the 12 B atoms in the supercell obtain enough energy and escape the supercell. Thus, a supercell shown in Fig. 8(b) is formed.
2) A Shockley partial dislocation with Burgers vector of $1/3\langle 1\bar{1}00\rangle$ slides across the (0002) lattice plane of the supercell. Then, a supercell shown in Fig. 8(c) is formed.
3) To maintain the symmetry and integrity of the hcp lattice of Mg, the lattice constants of a and c axes of the supercell shown in Fig. 8(c) must contract 3.9 and 29.9%, respectively. Finally, a unit cell of Mg is formed.

Since volume shrinkage is occurred due to the phase transformation, it is expected that elastic strain will be present in the phase transformation area. Further, the elastic strain can induce impurity segregation and drive crack tip through this area, which will have considerable effects on the mechanical properties of the materials.

4. Conclusions

(1) The MgB_2 phases are in-situ formed in the Mg alloy matrix composite reinforced with SiC whiskers and B_4C particles, through the chemical reactions, $B_4C + O_2 \rightarrow B_2O_3 + CO_2$ and $B_2O_3 + Mg \rightarrow MgB_2 + MgO$. The MgB_2 phases have hexagonal plate-like morphology with a remarkable interfacial energy anisotropy. The growth direction of the MgB_2 phases is the close-packed $\langle 11\bar{2}0\rangle$, instead of $\langle 0001\rangle$.

(2) Dislocation loop with Burgers vector of [0001] and 60° dislocation with Burgers vector of $1/3[2\bar{1}\bar{1}0]$ are observed in the MgB_2 phases. The (0001) interface

between MgB_2 and Mg is sharp without any intermediate layer. Misfit dislocations with regular arrangement are present at the interface.

(3) A phase transformation from MgB_2 to Mg is observed. A structural model is proposed to describe the phase transformation process.

Acknowledgements

This work was supported by the National Natural Sciences Foundation of China under Grand No. 59831020 and 59871055.

References

[1] W.M. Zhong, G. Lesperance, M. Suery, Meatll. Trans. 26A (1995) 2625.
[2] D.J. Lloyd, H. Lagace, A. Mcleod, P.L. Morris, Mater. Sci. Eng. A107 (1989) 73.
[3] M.V.an Den Burg, J.T.M. De Hosson, Acta Metal. Mater. 40(S) (1992) S281.
[4] X.G. Ning, J. Pan, K.Y. Hu, H.Q. Ye, Phil. Magn. A 66 (1992) 811.
[5] K. Wu, M.Y. Zhen, M. Zhao, C.K. Yao, Scr. Mater. 35 (1996) 529.
[6] R.J. Arsenault, Composites 25 (1994) 540.
[7] S.R. Nutt, J.M. Duva, Scr. Metall. 20 (1986) 1055.
[8] X.N. Zhang, D. Zhang, R.J. Wu, Z.G. Zhu, C. Wang, Scr. Mater. 37 (1997) 1631.
[9] Y.X. Chen, D.X. Li, G.D. Zhang, Scr. Mater. 43 (2000) 337.
[10] A. Brinkman, D. Mijatovic, G. Rijnders, V. Leca, H.J.H. Smilde, I. Oomen, A.A. Golubov, F. Roesthuis, S. Harkema, H. Hilgenkamp, D.H.A. Blank, H. Rogalla, Physica C 353 (2001) 1.
[11] J. Nagamatsu, N. Nakagawa, T. Muranaka, Y. Zenitani, J. Akimitsu, Nature 410 (2001) 63.
[12] S.Y. Oh, J.A. Cornie, K.C. Russell, Metall. Trans. 20A (1989) 533.
[13] Y.X. Chen, C.Y. Cui, L.L. He, J.T. Guo, D.X. Li, J. Mater. Res. 15 (2000) 1261.
[14] F.S. Shieu, S.L. Sass, Acta Metal. Mater. 38 (1990) 1653.